JOC The Journal of Organic Chemistry

Article

pubs.acs.org/joc

The Effect of Additives on the Zinc Carbenoid-Mediated Cyclopropanation of a Dihydropyrrole

Antonio Ramirez,* Vu Chi Truc,* Michael Lawler, Yun K. Ye, Jianji Wang, Chenchi Wang, Steven Chen, Thomas Laporte, Nian Liu, Sergei Kolotuchin, Scott Jones, Shailendra Bordawekar, Srinivas Tummala, Robert E. Waltermire, and David Kronenthal

Chemical Development, Bristol-Myers Squibb Company, One Squibb Drive, New Brunswick, New Jersey 0890, United States

Supporting Information

ABSTRACT: The synthesis of a key intermediate in the preparation of oral antidiabetic drug Saxagliptin is discussed with an emphasis on the challenges posed by the cyclopropanation of a dihydropyrrole. Kinetic studies on the cyclopropanation show an induction period that is consistent with a change in the structure of the carbenoid reagent during the course of the reaction. This mechanistic transition is associated with an underlying Schlenk equilibrium that favors the formation of monoalkylzinc carbenoid $IZnCH_2I$ relative to dialkylzinc carbenoid $Zn(CH_2I)_2$, which is responsible for the initiation of the cyclopropanation. The factors influencing reaction rates and diastereoselectivities are discussed with the aid of DFT computational studies. The rate accelerations observed in the presence of Brønsted acid-type additives correlate with the minimization of the undesired induction period and offer insights for the development of a robust process.

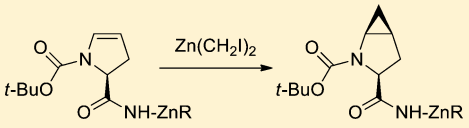

INTRODUCTION

Over the past two decades, 4,5-methanoprolines have evolved from peptidomimetic components of academic interest to privileged structures of relevance to the pharmaceutical industry. Following primary investigations by Urbach,[1] Pellicciari,[2] and Hanessian,[3] dozens of patents have covered the invention, development and uses of 4,5-methanoproline derivatives with diverse biological activities.[4] Approaches to the installation of the methano bridge exploit the cyclopropanation of dihydropyrrole precursors with halomethylzinc carbenoids. However, despite the proven utility of zinc carbenoid-mediated cyclopropanations and the extraordinary progress on the mechanistic understanding of these reactions, the implementation of these processes in an industrial setting is challenging. The notorious penchant of organozinc compounds for self-aggregation and equilibration, and for reacting with acidic substrates causes highly media- and substrate-dependent reactions. At the process development level, these attributes defy the application of unified mechanistic rationales to improve their outcome. On large scale, the common need of excess carbenoid to maximize conversion[5] and the limited reproducibility of the reactions[6] are often at odds with waste reduction objectives and stringent requirements on reproducibility, yield and purity.

Herein, we report mechanistic studies on the diastereoselective cyclopropanation of dihydropyrrole **1a** with $Zn(CH_2I)_2$[7] to give L-*cis*-4,5-methanoprolinamide **2**,[8] an intermediate in the preparation of the dipeptidyl peptidase IV inhibitor Saxagliptin (**3**, Scheme 1).[9] Kinetic studies demonstrate the existence of a detrimental induction period consistent with changes in the structure of the cyclopropanating reagent during the course of the reaction.[10] DFT computations based on experimental observations support a substrate-directed cyclopropanation with participation of the carboxamide moiety in **1a**. Notably, efforts toward process optimization revealed that the addition of substoichiometric amounts of TFA and water accelerates the cyclopropanation and enables the delivery of a reproducible, high-yielding process.

Scheme 1. Cyclopropanation of Dihydropyrrole 1a en Route to Saxagliptin

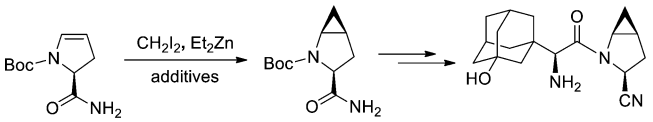

RESULTS AND DISCUSSION

Synthesis of Dihydropyrrole 1a. We preface the studies on the cyclopropanation with a brief description of efforts made to reduce the environmental impact and cost of the procedure to prepare dihydropyrrole **1a**.[11] The synthesis of **1a** transforms the commercially available ester **4**[12] into the corresponding carboxamide. It was essential to preserve the configuration of **4** and to generate crystalline intermediates that would upgrade purity and facilitate plant scale operations. The original procedure (Route A, Scheme 2)[13] starts with the basic hydrolysis of ester **4** followed by neutralization and isolation of its corresponding dicyclohexylammonium (DCHA) salt **5a**. Activation of the carboxylate with 4-(4,6-dimethoxy-1,3,5-triazin-2-yl)-4-methylmorpholinium chloride (DMT-MM)[14] and amidation with aqueous ammonia affords dihydropyrrole

Received: May 2, 2014
Published: June 10, 2014

   dx.doi.org/10.1021/jo500966m | J. Org. Chem. 2014, 79, 6233−6243

Scheme 2. Two Procedures for the Synthesis of Dihydropyrrole 1a

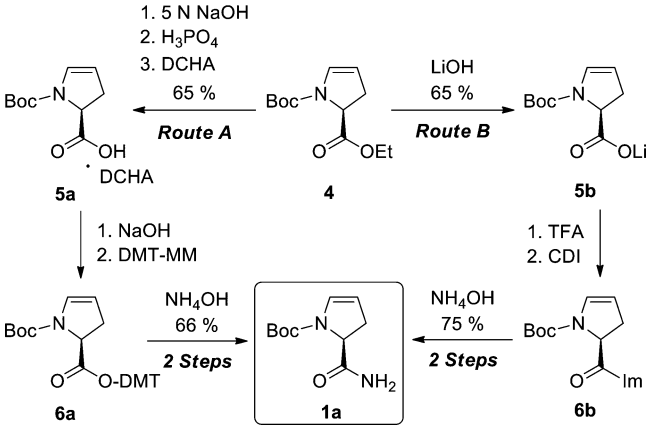

1a in 43% overall yield. Despite the satisfactory performance of these transformations, two noticeable aspects prompted a revision of the original route: (i) the molecular weight of DCHA in salt **5a**, and (ii) the expensive coupling reagent DMT-MM. A combination of salt screening and solvent optimization led to the identification of a crystalline form of the lithium carboxylate **5b**. Likewise, the examination of a variety of coupling reagents and reaction conditions enabled the substitution of DMT-MM with 1,1′-carbonyldiimidazole (CDI). These changes resulted in a superior yield for the two-step sequence, leading to dihydropyrrole **1a** from **5b** (49% overall yield; Route B, Scheme 2). Details for the conversion of ester **4** into dihydropyrrole **1a** are given in the Experimental Section.

Cyclopropanation of Dihydropyrrole 1a with Zn(CH_2I)$_2$: General Aspects. Next, we investigated the cyclopropanation of dihydropyrrole **1a** with halomethylzinc reagents conveniently generated in situ[15] by adding variable amounts of Et_2Zn and CH_2I_2 to a solution of **1a** in AcOEt.[16] The sequential treatment of **1a** with 1 equiv of Et_2Zn and 1 equiv of CH_2I_2 resulted in very low yields (ca. 5%) of the cyclopropanated product **2** after extended reaction times (ca. 18 h at 20 °C). Increasing the Et_2Zn charge to 2 equiv and adding 1 equiv of CH_2I_2 gave the desired product in slightly higher, but still poor, yields (ca. 20%). Gratifyingly, the reaction proceeded with 2 equiv of Et_2Zn and 2 equiv of CH_2I_2 to afford 4,5-methanoprolinamide **2** in 72% yield and 40:1 *dr*. The excellent diastereoselectivity of the cyclopropanation is consistent with a *syn* delivery of the carbenoid by the carboxamide group.[17] On the basis of these results, we assumed that the first equivalent of Et_2Zn reacts with **1a** to afford zinc amidate **7a**, and that the addition of 2 equiv of CH_2I_2 to this mixture was required to generate the cyclopropanating reagent (Scheme 3). Considering the various alkylzinc species present, a number of possible reagents could be envisioned: (i) Zn(CH_2I)$_2$ (Wittig reagent, Path A in Scheme 3), (ii) a mixture of iodomethylzinc amidate **8a** and $EtZnCH_2I$ (Furukawa reagent, Path B in Scheme 3),[18] and (iii) combinations of Zn(CH_2I)$_2$, amidate **8a**, and $EtZnCH_2I$ that could result from the coexistence of paths A and B or from the dynamic alkyl group exchange between the different Zn-bearing species in solution.[19] The formation of **7a** upon treatment of **1a** with 1 equiv of Et_2Zn was evidenced by (i) gas evolution during the addition of the first equiv of Et_2Zn that subsided throughout the charge of further equivalents,[20] (ii) the diagnostic shift of the carboxamide IR band of **1a** to

Scheme 3. Plausible Reactions of Dihydropyrrole 1a with 2 equiv of Et_2Zn and CH_2I_2

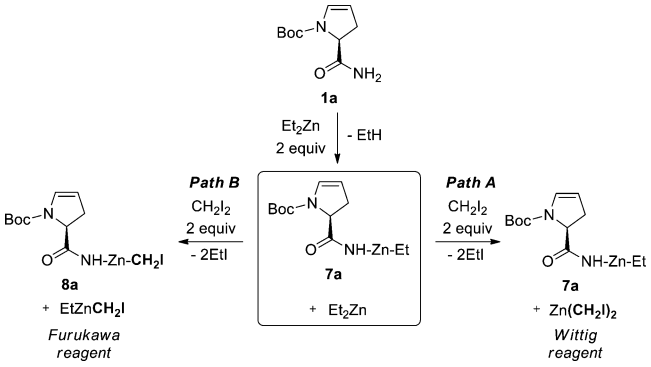

lower frequency[21] (from 1685 to 1580 cm^{-1}), and (iii) the downfield migration of the carboxamide ^{13}C NMR signal of **1a** (from 174.6 to 181.6 ppm).[22] The addition of 1 equiv of Et_2Zn to **1a** also caused partial changes in the original IR band of the *tert*-butyl carbamate (from 1710 cm^{-1} to bands coexisting at 1710 and 1620 cm^{-1}), which could be traced to coordination of the carbamate to the Zn atom in a chelated version of **7a** (vide infra). The IR frequencies and ^{13}C NMR chemical shifts of **7a** were insensitive to the charge of a second equiv of Et_2Zn or the addition of $Zn(CH_2I)_2$.

To understand the marked dependence of the cyclopropanation yields on the relative stoichiometries of Et_2Zn, CH_2I_2 and **1a**, we explored the reaction between CH_2I_2 and the saturated zinc amidate **7b**, an unreactive surrogate for amidate **7a** generated from pyrrolidine **1b** (eq 1).[13] Cursory ^1H NMR

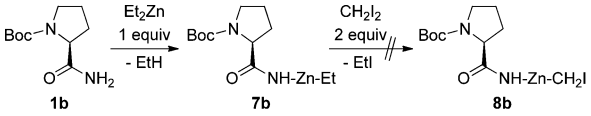

(1)

analyses of samples containing (i) 1 equiv of Et_2Zn and 2 equiv of CH_2I_2 as the control reaction, or (ii) 1 equiv of amidate **7b** and 2 equiv of CH_2I_2, revealed the exclusive formation of EtI in the control experiment containing Et_2Zn.[23] To gain further insight, we examined the consumption of CH_2I_2 through its deuterated analogue CD_2I_2 using in situ ReactIR; the effect of isotopic substitution enabled a clear inspection of the C–D bond stretches corresponding to CD_2I_2 (2310 and 2190 cm^{-1})[24] and the associated Zn carbenoids (2160 cm^{-1}). Monitoring the absorbance of CD_2I_2 at 2310 cm^{-1} confirmed the unanticipated stability of CH_2I_2 in the presence of amidate **7b**: whereas 2 equiv of CD_2I_2 were immediately consumed by 1 equiv of Et_2Zn under the control conditions, 2 equiv of CD_2I_2 remained unchanged upon their treatment with 1 equiv of **7b** (eq 1). These observations suggest that the failure of the direct cyclopropanation of **7a** with CH_2I_2 stems from the inability of the ethyl zinc amidate to form an active cyclopropanating reagent (Scheme 3).[25]

Next, we examined the reaction of CH_2I_2 with 1:1 mixtures of amidate **7b** and Et_2Zn (eq 2). ^1H NMR and ReactIR spectroscopic studies revealed that, in contrast to the lack of reactivity observed for **7b** alone, solutions containing equimolar amounts of **7b** and Et_2Zn react with 1 or 2 equiv of CH_2I_2 as demonstrated by the presence of EtI in the ^1H NMR spectra and the rapid decay of the CD_2I_2 absorbance on the ReactIR in the deuterated series. Interestingly, addition of a third

dx.doi.org/10.1021/jo500966m | J. Org. Chem. 2014, 79, 6233–6243

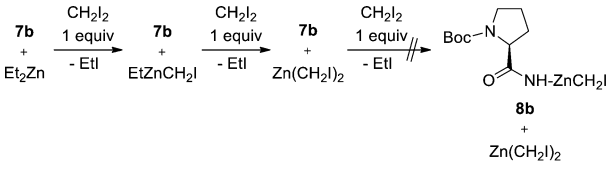

(2)

equivalent of CD_2I_2 did not cause further spectroscopic changes after the consumption of the first 2 equiv. These results suggest that the differences between the cyclopropanation of 1:1 mixtures of **7a** and Et_2Zn with 1 equiv of CH_2I_2 versus 2 equiv of CH_2I_2 arise from the limited reactivity of the cyclopropanating species that were formed under the reaction conditions. In addition, the reluctance displayed by 1:1:2 combinations of **7b**, Et_2Zn and CH_2I_2 to react with a third equivalent of CH_2I_2 suggests that **7b** cannot react with CH_2I_2 or participate in exchange with the iodomethyl groups of $Zn(CH_2I)_2$ (eq 3).[26] ^{13}C NMR spectra of 1:1:1 mixtures of **7b**,

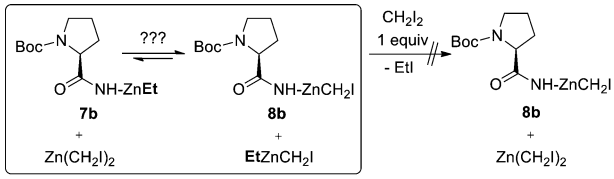

(3)

Et_2Zn, and $^{13}CH_2I_2$ exhibited a complex array of broad signals indicative of the coexistence of several iodomethylzinc species.[18] In contrast, ^{13}C NMR spectra of 1:1:2 mixtures of **7b**, Et_2Zn, and $^{13}CH_2I_2$ displayed a single broad resonance in the $ZnCH_2I$ region (δ −16.6 ppm) consistent with the formation of $Zn(CH_2I)_2$.[27]

The tendency of organozinc compounds to self-aggregate adds an additional layer of complexity to the analysis of the reaction. Literature precedents document that zinc-based cyclopropanating reagents have a propensity to exist as monomers,[15,28] whereas zinc amidates are particularly prone to form higher structural ensembles.[29] ^1H and ^{13}C NMR spectra of samples containing **7a** displayed broad signals that pointed toward the likely aggregation of the zinc amidate species. IR spectra of samples with varying concentrations of **7a** revealed marked differences in the relative intensities of the IR bands, consistent with the existence of more than one aggregate of **7a** in solution (Figure 1).[30] Unfortunately, our efforts to ascertain the aggregation state of amidate **7a** by cryoscopic methods were repeatedly thwarted by its poor solubility and stability. The existence of **7a** as a reactive mixture of aggregates will resurface as a source of mechanistic complexity in the context of the kinetic studies discussed below.

Building on spectroscopic and reactivity observations, we turned to DFT calculations to evaluate the structure of **7a** in the presence of $Zn(CH_2I)_2$ using the B3LYP method and the 6-311+G(2d,2p) basis set for all the atoms except iodine.[32] Combinations of plausible conformers and solvation numbers were tested, and the optimized structures were submitted to single point calculations using the same basis set and incorporating PCM corrections for AcOEt as the solvent. Relevant structures and relative energies obtained from balanced equilibria are summarized in Figure 2, where *S*

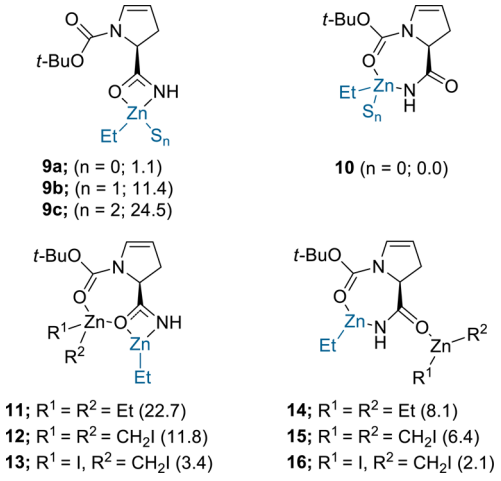

Figure 2. Plausible structures for monomeric zinc amidate **7a** and its complexes with Et_2Zn, $Zn(CH_2I)_2$, and $IZnCH_2I$. The calculated relative energies ($\Delta G^{\ddagger}$, kcal·mol^{-1}) are given in parentheses.

represents the coordinating solvent AcOEt, and *n* defines the solvation number.[33] The calculations on the most stable monomeric forms of **7a** (i.e., **9** and **10**) suggest that the 7-membered chelate in **10** is marginally stabilizing relative to the η^3-complexed monomer **9a** (~1 kcal/mol) and that solvation is destabilizing despite the three-coordinate zinc atom present in the unsolvated species.[34] Moreover, in agreement with the resilience demonstrated by the IR and ^{13}C NMR spectra of zinc amidate **7a** in the presence of Et_2Zn or $Zn(CH_2I)_2$, the calculations predict that complexation of the carbenoid reagents to zinc amidates **9** or **10** is unfavorable. Coordination of the

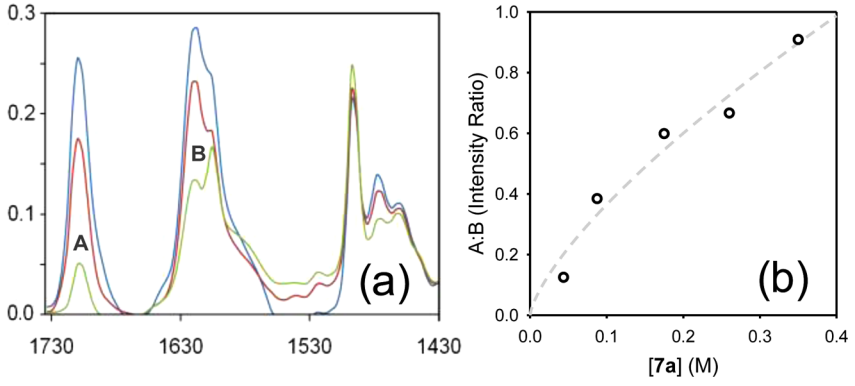

Figure 1. (a) Representative IR spectra of **7a** recorded at different concentrations using [AcOEt] = 5.5 M in toluene at 20 °C: [**7a**] = 0.35 M (blue); [**7a**] = 0.26 M (red); [**7a**] = 0.09 M (green). (b) Plot of the intensity ratios for the IR bands A (1710 cm^{-1}) and B (1620 cm^{-1}) versus [**7a**].[31]

dx.doi.org/10.1021/jo500966m | J. Org. Chem. 2014, 79, 6233−6243

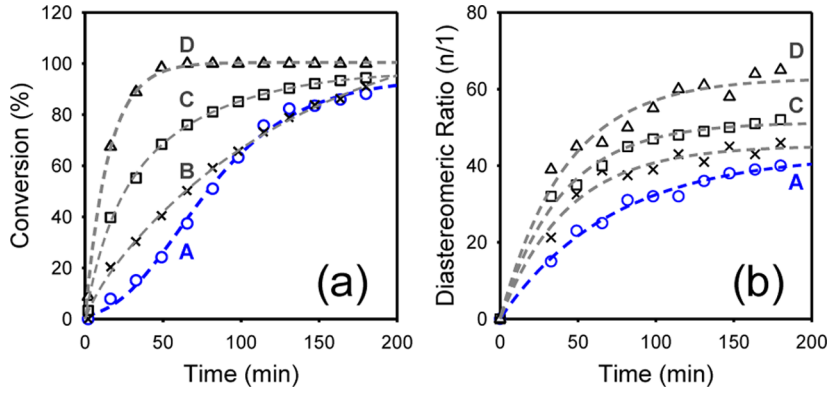

Figure 3. (a) Plot of conversion versus time for the cyclopropanation of **7a** (0.24 M) with $Zn(CH_2I)_2$ (0.26 M) at 20 °C in the presence of various amounts of ZnI_2: (A) no ZnI_2; (B) 0.10 equiv ZnI_2; (C) 0.15 equiv ZnI_2; (D) 0.20 equiv ZnI_2. (b) Plots of the *syn*/*anti* diastereomeric ratios versus time for the reactions in panel a.

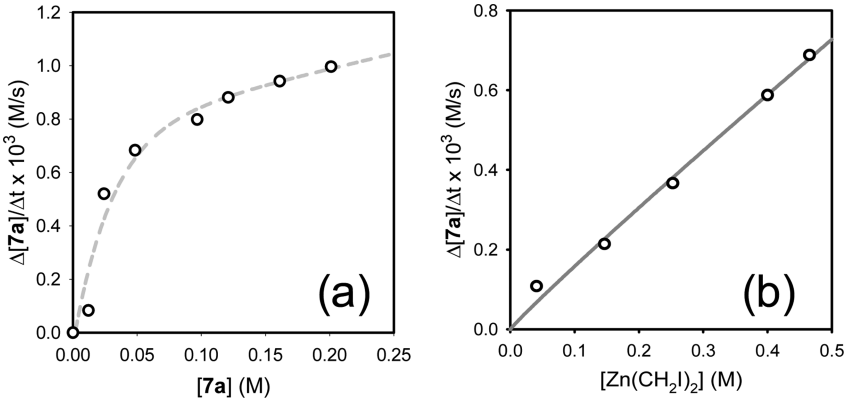

Figure 4. (a) Plots of k_{obsd} for the cyclopropanation of **7a** by $Zn(CH_2I)_2$ at 0 °C versus (a) [**7a**], (b) $[Zn(CH_2I)_2]$. Rate dependencies on $[Zn(CH_2I)_2]$ and [**7a**] were measured using [AcOEt] = 5.2 M in toluene. Rate dependencies on $[Zn(CH_2I)_2]$ were measured using [**7a**] = 0.048 M. Rate dependencies on [**7a**] were measured using $[Zn(CH_2I)_2]$ = 0.465 M.

most Lewis acidic species $IZnCH_2I$ to give structure **16** is favored over complexation of $Zn(CH_2I)_2$ or $ZnEt_2$ to give structures **15** and **14**, respectively.

Cyclopropanation of Dihydropyrrole 1a with Zn-$(CH_2I)_2$: Rate Studies. Monitoring the cyclopropanation of **7a** with $Zn(CH_2I)_2$ at 20 °C by HPLC analysis revealed the presence of an induction period (Figure 3a, curve A) reminiscent of the autocatalytic profile observed by Denmark and co-workers in the cyclopropanation of allylic alcohols.[18b,35] In their work, the source of this behavior was elegantly traced back to the occurrence of a Schlenk equilibrium between $Zn(CH_2I)_2$ and $IZnCH_2I$ (Simmons-Smith reagent, eq 4) promoted by the ZnI_2 that is formed during the cyclopropanation (eqs 5 and 6). The authors concluded that the equilibrium favors the $IZnCH_2I$ species, which in turn is the most active cyclopropanating reagent. To corroborate the influence of the Schlenk equilibrium in the cyclopropanation of **7a** with $Zn(CH_2I)_2$, we monitored the reaction in the presence of ZnI_2. Adding ZnI_2 to a mixture of equimolar amounts of **7a** and $Zn(CH_2I)_2$ eliminated the induction period and promoted a faster conversion (e.g., the initial rates analysis of curves A and D in Figure 3a affords a $k_{rel} \sim 30$). The addition of increasing amounts of ZnI_2 further enhanced the rate of the process (cf. curves B and C in Figure 3a).[36]

$$\frac{1}{2}Zn(CH_2I)_2 + \frac{1}{2}ZnI_2 \rightleftharpoons IZnCH_2I \quad (4)$$

$$\text{olefin} + Zn(CH_2I)_2 \rightarrow \text{cyclopropane} + IZnCH_2I \quad (5)$$

(e.g., **7a**)

$$\text{olefin} + IZnCH_2I \rightarrow \text{cyclopropane} + ZnI_2 \quad (6)$$

Plotting the *syn*/*anti* diastereomeric ratios of the cyclopropanated product **2** versus time reveals an improvement of the diastereoselectivity as the reaction progresses. For example, in the absence of added ZnI_2, the diastereomeric ratio at 15% conversion is approximately 15:1, whereas at 90%, conversion the diastereomeric ratio grows to ~40:1. Interestingly, the lowest diastereoselectivities correspond to the cyclopropanation mediated by $Zn(CH_2I)_2$ (*dr* ~ 40:1, Figure 3b, curve A), and addition of ZnI_2 leads to enhanced diastereomeric ratios (dr ~ 60:1, Figure 3b, curve D). These observations are consistent with the concurrence of mechanisms described by eqs 4−6, and suggest that the improvement of the diastereoselectivities derives from the cyclopropanation mediated by $IZnCH_2I$.

To gain further insight into the induction period, we carried out kinetic studies on the cyclopropanation of zinc amidate **7a** using the method of initial rates.[37] Stock solutions of **7a** and $Zn(CH_2I)_2$ were combined at 0 °C and the formation of **2** monitored relative to an internal standard by HPLC. The reactions displayed a clean decay of dihydropyrrole **1a** and the simultaneous formation of the cyclopropanated product **2**. Monitoring the growth of **2** over a range of zinc amidate **7a** and $Zn(CH_2I)_2$ concentrations provided a complex dependence on

dx.doi.org/10.1021/jo500966m | J. Org. Chem. 2014, 79, 6233−6243

the concentration of **7a** and a first-order dependence on the concentration of $Zn(CH_2I)_2$ (Figure 4).[38] The complex rate dependence on the concentration of **7a** most likely reflects the existence of a changeable, concentration-dependent distribution of amidate aggregates that can undergo cyclopropanation (Figure 1). A plausible mechanism is represented by the general rate-determining steps in eqs 7 and 8, where *m* denotes aggregate numbers for productive forms of **7a**, and *n* defines aggregate fractions that react via a coexisting pathway.

$$(\mathbf{7a})_m + Zn(CH_2I)_2 \rightarrow [(\mathbf{7a})_m Zn(CH_2I)_2]^{\ddagger} \quad (7)$$

$$\frac{1}{n}(\mathbf{7a})_m + Zn(CH_2I)_2 \rightarrow [(\mathbf{7a})_{m/n} Zn(CH_2I)_2]^{\ddagger} \quad (8)$$

The initial rates and the concentration dependence on ZnI_2 depict two components of a changing mechanistic scenario guided by the formation of ZnI_2 during the reaction. At the onset, $Zn(CH_2I)_2$ engages in a slow cyclopropanation and the Schlenk equilibrium described in eq 4 has a low impact. As the levels of ZnI_2 increase, the Schlenk equilibrium plays an active role and opens a new cyclopropanation pathway dominated by $IZnCH_2I$, the most reactive cyclopropanating species. In the absence of structural data on the aggregation states of zinc amide **7a**, however, eqs 5−8 represent elementary pathways rather than actual mechanisms.

Evaluation of the Reaction Pathways: DFT Calculations. We explored plausible transition structures for the cyclopropanation of **7a** using DFT calculations. A series of geometries were examined for both reactants and transition structures, saddle points were confirmed by the occurrence of a single imaginary frequency, and intrinsic reaction coordinate calculations (IRC) were performed from the transition states to confirm the lowest energy reaction pathways that connect the corresponding minima. Transition structures are represented in Figure 5. Additional data are included in Supporting Information. Free energies of activation ($\Delta G^{\ddagger}$, kcal/mol) are arbitrarily related to structure **10** (*n* = 0, Figure 2). **TS1** and **TS2** denote transition structures featuring $Zn(CH_2I)_2$ and $IZnCH_2I$ as the cyclopropanating reagents, respectively. *Syn* cyclopropanations are classified into two series depending on whether the EtZnNH group of amidate **7a** coordinates to the zinc carbenoid (series a) or is engaged in a 7-membered ring (series b); *anti* cyclopropanations are represented by series c. The discussion will focus on three aspects: (i) the nature of the rate-determining transition structures, (ii) the differences between $Zn(CH_2I)_2$ and $IZnCH_2I$ as cyclopropanating reagents, and (iii) the origins of diastereoselectivity. All the transition structures display geometries that correspond to a methylene transfer mechanism rather than a carbometalation.[39] In general, the cyclopropanation occurs via an asynchronous process in which the position C4 of the amidate **7a** displaces the iodine atom of the iodomethylene moiety while the carbenoid center dissociates from the Zn atom to form the products. The iodine substitution takes place via a S_N2-like arrangement with C−C−I angles >160°. The higher activation barriers calculated for the $Zn(CH_2I)_2$-based cyclopropanations (i.e., **TS1**) relative to those mediated by $IZnCH_2I$ (i.e., **TS2**) are consistent with the rate accelerations experimentally observed under conditions that favor the formation of $IZnCH_2I$. Inspection of the geometries associated with **TS1b** and **TS2b** suggest that the superiority of $IZnCH_2I$ correlates with angle strain (Figure 6). Whereas the Zn center bound to a single alkyl group in **TS2b** may comfortably adopt a tetrahedral hybridization by coordinating the amidate moiety and two iodine atoms, the Zn connected to two alkyl groups in **TS1b** suffers a destabilizing deviation from the 180° R−Zn−R bond angle believed to be optimal for dialkylzinc reagents[40] upon coordination to the amidate group. In addition, the computations corroborate a preference for *syn* cyclopropanation: structures **TS1b** and **TS2b** with the amidate moiety bound to the cyclopropanating reagent are more stable than their *anti* analogues **TS1c** and **TS2c**. Among the *syn* structures, those involving the EtZnNH group in a 7-membered chelate are preferred (series b). The differences between the activation energies calculated for the *syn* and *anti* $IZnCH_2I$-based cyclopropanations (i.e., **TS2b** versus **TS2c**, $\Delta G^{\ddagger}$ = 1.6 kcal/mol) compared with the differences calculated for the *syn* and *anti* cyclopropanations promoted by $Zn(CH_2I)_2$ (i.e., **TS1b** versus **TS1c**, $\Delta G^{\ddagger}$ = 1.2 kcal/mol) are in qualitative agreement with the enhanced diastereoselectivity offered by $IZnCH_2I$. The superior selectivity of $IZnCH_2I$ is presumably due to a strengthened C═O−ZnI interaction associated with the higher Lewis acidity of the Zn center of $IZnCH_2I$ and the concomitant stabilization of the leaving ZnI_2 in the emerging RNHZn−IZnI substructure.

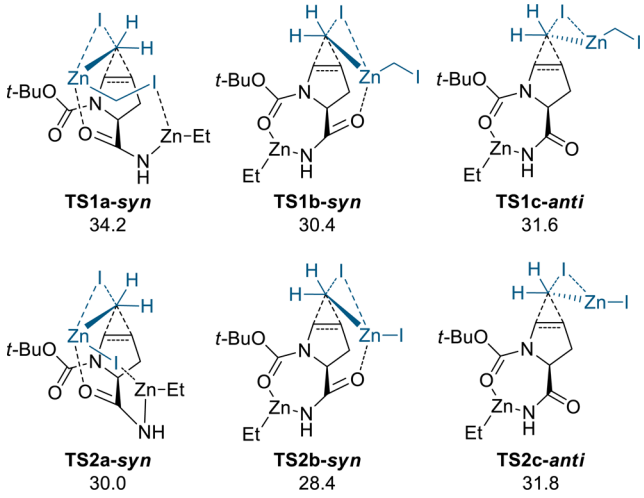

Figure 5. Plausible transition structures **TS1** and **TS2**. The calculated relative energies ($\Delta G^{\ddagger}$, kcal·mol^{-1}) are also given.

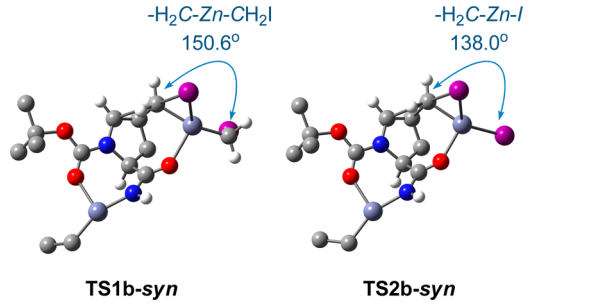

Figure 6. Transition structures for the *syn* cyclopropanations calculated with DFT.

A Search for Alternative Additives to ZnI_2. With the aim of circumventing the incomplete conversions observed in the absence of ZnI_2 (curve A, Figure 3a) and finding an economical alternative to ZnI_2,[41] we investigated the use of acyloxy-

dx.doi.org/10.1021/jo500966m | J. Org. Chem. 2014, 79, 6233−6243

substituted carbenoids (i.e., RCO_2ZnCH_2I)[42] by treating equimolar mixtures of zinc amidate **7a** and $Zn(CH_2I)_2$ with Brønsted acids AcOH or TFA. The enhanced reactivity of acyloxy-substituted carbenoids and the ease of preparation in situ[43] made the use of these additives an attractive option for implementation on scale. The results are summarized in Table 1 and Figure 7. We were pleased to find that with

Table 1. Effect of Brønsted Acid-Type Additives on the Cyclopropanation of Dihydropyrrole 1a with $Zn(CH_2I)_2$

entry	additive[a,b]	equiv	conv (18 h)	yield (%)[c]	dr (*syn*/*anti*)[d]
1	–	–	88%	72%	40:1
2	AcOH	0.2	93%	75%	40:1
3	TFA	0.2	100%	86%	40:1
4	water	0.2	97%	88%	50:1
5	AcOH/water	0.5/0.2	100%	88%	45:1
6	TFA/water	0.5/0.2	100%	95%	45:1

[a]Water (0.2 equiv) was added to a solution of **1a** (1.0 equiv) in AcOEt and the resulting mixture was sequentially treated with Et_2Zn (2.1 equiv) and CH_2I_2 (2.0 equiv) under the conditions indicated in the Experimental Section. [b]Additives other than water were introduced following the in situ formation of zinc amidate **7a** and $Zn(CH_2I)_2$. [c]Yields determined by HPLC analysis versus a calibrated internal standard. [d]Diastereomeric ratios (dr) determined by HPLC analysis at the end of the reaction. Value not determined.

substoichiometric amounts of AcOH or TFA cyclopropanations were faster and achieved a higher level of conversion relative to the reactions carried out in the absence of additives (entries 2 and 3, Table 1; curve A, Figure 7a). Plots of the reaction progress versus time revealed profiles that could not be fit to a second-order kinetics and contained initial curvatures with a minor sigmoidal component (curves B–C, Figure 7a). Moreover, diastereomeric ratios changed during the process affording values similar to those observed for the cyclopropanation without additives (dr ~ 40:1 at completion, Figure 7b). These results suggested the existence of a complex mechanism that could minimize the distinct induction period observed in the absence of additives.

To investigate the role of the acidic additives, we turned to IR and ^{13}C NMR spectroscopy. Adding 0.2 equiv of AcOH or TFA to solutions containing 1 equiv of surrogate **7b** and 1 equiv of $Zn(CD_2I)_2$ (1 equiv of $Zn(^{13}CH_2I)_2$ for the NMR studies) occurred with gas evolution and simultaneous changes on the IR and ^{13}C NMR signals diagnostic of the zinc amidate group (1580 cm^{-1} and 181.6 ppm, respectively). Contrary to our expectations, the IR and ^{13}C NMR signals of the carbenoid (2160 cm^{-1} and −16.6 ppm, respectively) remained unchanged and ^1H NMR spectra demonstrated the absence of resonances corresponding to MeI. The spectroscopic studies implied the reaction of the acids with the EtZn-amidate moiety of **7a** rather than the $Zn(CH_2I)_2$ carbenoid to give RCO_2Zn-amidates represented by **8a** in eq 9. We deduce that changes to the

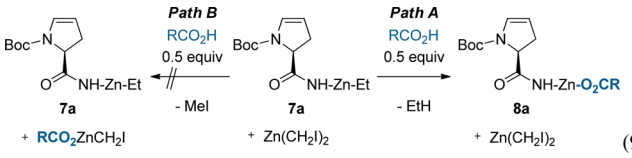

(9)

nature of the directing group or the aggregation state of the zinc amidate account for the changes observed in the performance of the reaction (eqs 10 and 11).

$$\mathbf{8a} + Zn(CH_2I)_2 \rightarrow \text{cyclopropane} + IZnCH_2I \quad (10)$$

$$\mathbf{8a} + IZnCH_2I \rightarrow \text{cyclopropane} + ZnI_2 \quad (11)$$

In the course of these studies, we also discovered a noticeable increase of the initial rates and diastereoselectivities when the AcOEt solvent was marginally wet. Varying levels of moisture appeared to correlate with a lack of reproducibility suggesting that the reaction of Et_2Zn with water during the formation of zinc amidate **7a** influenced the outcome of the cyclopropanation. A study of the tolerance of the cyclopropanation for moisture indicated that, in the reaction with 2.1 equiv of Et_2Zn and 2.1 equiv of CH_2I_2, the rates improved within a range of 0.05–0.2 equiv of water, leveled off at ca. 0.2 equiv, and decreased slightly with 0.4 equiv of water. The acceleration of reactions mediated by Et_2Zn in the presence of catalytic amounts of water has been attributed to the formation of ZnO complexes[44,45] that can transform the structure of the reactants,[42d,46] catalyze the cyclopropanation acting as Lewis acids,[28a,47] or both. We obtained indirect support for the catalytic capacity of related Lewis acidic species by monitoring the cyclopropanation rates in the presence of ZnO. Although the poor solubility of ZnO in the reaction medium prevents a rigorous analysis of the kinetic profile, its presence eliminated

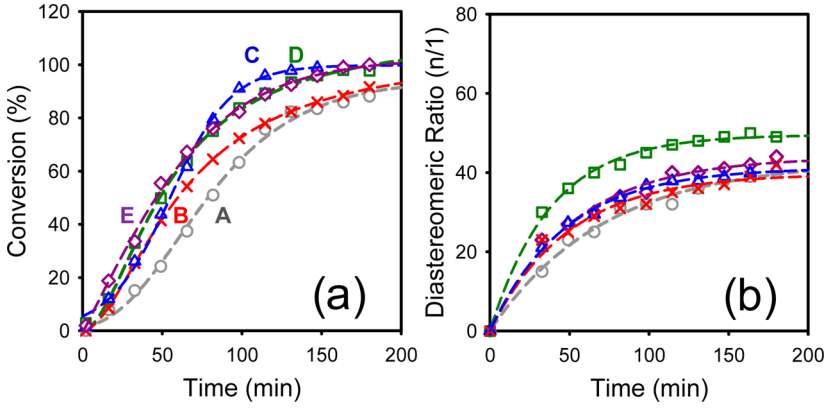

Figure 7. (a) Plot of conversion versus time for the cyclopropanation of **7a** (0.24 M) with $Zn(CH_2I)_2$ (0.26 M) at 20 °C in the presence of various additives: (A) no additive; (B) 0.2 equiv AcOH; (C) 0.2 equiv TFA; (D) 0.2 equiv H_2O; (E) 0.2 equiv TFA and 0.2 equiv H_2O. (b) Plots of the *syn*/*anti* diastereomeric ratios versus time for the reactions in panel a.

dx.doi.org/10.1021/jo500966m | J. Org. Chem. 2014, 79, 6233–6243

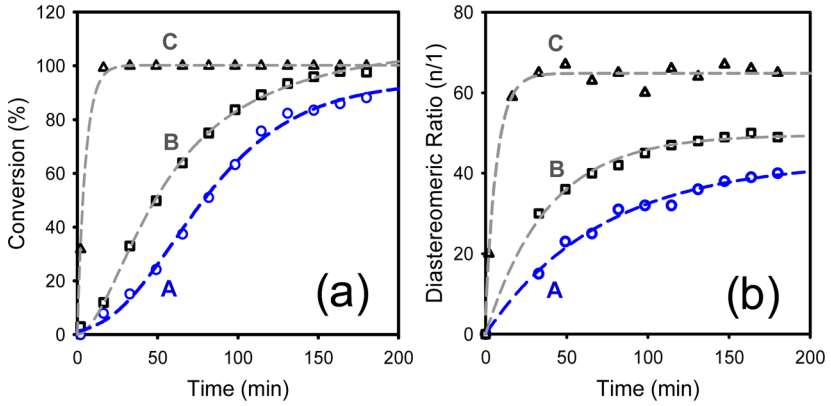

Figure 8. (a) Plot of conversion versus time for the cyclopropanation of **7a** (0.24 M) with $Zn(CH_2I)_2$ (0.26 M) at 20 °C in the presence of various additives: (A) no additive; (B) 0.2 equiv water; (C) 0.2 equiv ZnO. (b) Plots of the *syn*/*anti* diastereomeric ratios versus time for the reactions in panel a.

the induction period to afford rates that were superior to those observed with AcOH, TFA, or water (curve C, Figure 8a). In addition, the diastereoselectivities changed with the course of the reaction and reached the highest values measured for the cyclopropanation (dr ~ 60:1, curve C, Figure 7b). The results are in reasonable accord with the catalytic properties of ZnO[48] and can offer an explanation to the accelerating effect of water as far as Et_2Zn forms related ZnO complexes under the reaction conditions. Clearly, however, the superior rates measured in the presence of ZnO (e.g., the initial rates analysis of curves A and C in Figure 8a provides a k_{rel} ~ 10) and the limited window of benefit observed within a range of water equivalents forewarn of mechanistic complexity.

Given the improved kinetic profiles and conversions obtained with the introduction of acidic additives and water, further screening of acid and water loadings identified optimal conditions that resulted in the use of 0.2 equiv of water prior to the addition of Et_2Zn and 0.5 equiv of TFA after the formation of the $Zn(CH_2I)_2$ carbenoid (entry 6, Table 1). These conditions curbed the induction period, afforded high yields and selectivities, and provided levels of reproducibility that could not be accomplished in the absence of the additives. As a result, they were chosen to implement the cyclopropanation of **1a** on scale (Scheme 4, see Experimental Section).

Scheme 4. Optimized Cyclopropanation of Dihydropyrrole 1a

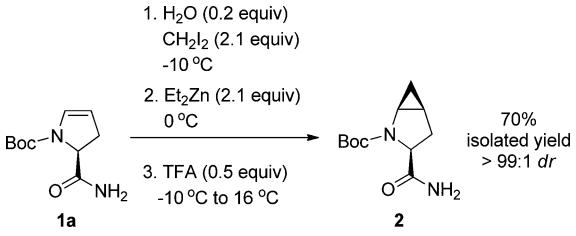

CONCLUSION

The development of a scalable route to prepare L-*cis*-4,5-methanoprolinamide (**2**) resulted in the formulation of a robust process that delivered superior yields and diastereoselection. Early steps were revised to preserve the configuration of the stereochemically labile starting material **4**, and facilitate the manufacturing process by introducing a sustainable crystalline form of carboxylate **5** (Scheme 2). Of central importance to the process was the mechanistic evaluation of the cyclopropanation of dihydropyrrole **1a**, which identified the need to circumvent a problematic induction period. Kinetic and structural studies supported a scenario characterized by the coexistence of at least two reaction pathways. At the onset, $Zn(CH_2I)_2$ is the major cyclopropanating species and promotes a slow reaction with moderate diastereoselectivity. As the reaction proceeds, the reaction becomes faster and more diastereoselective. The mechanistic transition is associated with an underlying Schlenk equilibrium that favors the more reactive cyclopropanating reagent $IZnCH_2I$. Computational studies depicted a methylene transfer characterized by the S_N2-like attack of the alkene to the carbenoid followed by ring closure and departure of the IZnR group (R = $-CH_2I$ or $-I$). Faster and more diastereoselective cyclopropanations mediated by $IZnCH_2I$ originate from a selective stabilization of the *syn* transition structures relative to the corresponding ground states. Presumably, simultaneous coordination of the Lewis basic zinc amidate to the Lewis acid $IZnCH_2I$ reagent and the ZnI_2 leaving species in the transition state is favored relative to the coordination of the zinc amide to the $Zn(CH_2I)_2$ reagent and the $IZnCH_2I$ leaving group.

Experiments originally intended to study the consequences of modifying the structure of the $Zn(CH_2I)_2$ carbenoid by adding Brønsted acids revealed even greater levels of complexity. In particular, the addition of TFA and water provided a practical acceleration by modifying the structure of the zinc amidate and forming zinc oxo-complexes, respectively. In a research area infused with new zinc carbenoid-based reagents, these results indicate that changes in the structure of the substrate or the nature of the organozinc components can also lead to sizable improvements. Structural evidence for the aggregation of zinc amidate **7a** in solution as well as kinetic support for the occurrence of an aggregate-based cyclopropanation suggest plausible scenarios in which the addition of Lewis acidic zinc salts may not only catalyze the putative cyclopropanation transition states but also affect Schlenk-type equilibria and aggregation pathways at the ground state level.

More than 50 years after the seminal reports by Simmons and Smith on the diastereoselective cyclopropanation of allylic alcohols,[49] advances in mechanistic understanding continue to expose the complexities of a substrate-controlled reaction that is moisture-sensitive and has a propensity for ligand exchange, aggregation, and equilibration effects. Although studies on the substrate-directed cyclopropanation of allylic amines and

dx.doi.org/10.1021/jo500966m | J. Org. Chem. 2014, 79, 6233−6243

amides are less common, the general trends exhibited by allylic alcohols seem to apply: rates and selectivities arise from a diverse array of competing mechanisms that are strongly influenced by reaction conversion. The uncertainty lurking in the background of these processes contributes to the challenges encountered in their scaleup and demands greater diligence in a manufacturing setting where process robustness is compulsory. The studies reported herein provided a foundation to improve the performance and reproducibility of a zinc carbenoid-mediated cyclopropanation. Perhaps more importantly, these studies underscore the need to gain fundamental understanding of even the most generic transformations if robustness and high reproducibility is our goal.

EXPERIMENTAL SECTION

General Information. AcOEt and toluene >99.8% pure by GC analysis were dried over molecular sieves and their water contents determined by coulometric Karl Fischer titration (H_2O <0.005%). Et_2Zn stock solutions in toluene were titrated for active base using literature methods.[50] CH_2I_2 and CD_2I_2 >99.0% pure were filtered through carbon a pad (zeta pad R30SPG60) and used immediately. All the materials were manipulated under nitrogen using standard vacuum line and syringe techniques.[51] All reactions were performed under an inert atmosphere of dry nitrogen in 20 mL oven-dried vials fitted with TFE septa. Gas-tight syringes were used to transfer moisture-sensitive solutions. Reaction samples quenched with 0.05% TFA in ACN were analyzed on a HPLC system equipped with a C18 column (4.6 × 150 mm) and a SPD-20A/20AV UV-VIS detector. ^{1}H NMR and ^{13}C NMR spectra were recorded on a 400 MHz spectrometer in $CDCl_3$ unless stated otherwise. Chemical shifts for ^{1}H and ^{13}C NMR spectra are reported in parts per million downfield from TMS. NMR data are represented as follows: chemical shift (δ, ppm), multiplicity (s = singlet, d = doublet, t = triplet, m = multiplet, bs = broad signal), coupling constants (J, Hz), and integration. Infrared spectra were obtained in CH_2Cl_2 using a ReactIR fitted with a Sentinel probe within a spectral range of 4000−650 cm^{-1}.

Preparation of Lithium (2*S*)-1-(*tert*-Butoxycarbonyl)-2,3-dihydro-1*H*-pyrrole-2-carboxylate (5b). A solution of ester **4**[12] (6.0 g, 24.8 mmol) in *i*-PrOH (24 mL) and 4 N aqueous LiOH (6.6 mL) was heated to 50 °C for 3 h. After cooling the mixture to rt, it was filtered and concentrated via vacuum distillation to 23.0 mL while maintaining the temperature below 45 °C. Toluene (50 mL) and *i*-PrOH (9 mL) were added, and the mixture was concentrated to 35 mL following the same protocol as before. *i*-PrOH (6.5 mL) and water (0.4 mL) were added to the resulting slury, and the mixture was aged for 1 h at 40 °C. The mixture was then diluted with *n*-heptane (20 mL), cooled to 0−5 °C over 2 h, and aged for 2 h at the same temperature. The precipitate formed was collected, washed with a mixture consisting of *i*-PrOH and *n*-heptane (1:8, vol/vol), and dried in vacuo to provide a white solid (3.54 g, 65%); mp 117 °C (DSC); IR (DMSO) 1698, 1625 (C═O) cm^{-1}; ^{1}H NMR (400 MHz, DMSO-d_6; major rotamer) δ: 6.44 (bs, 1H), 4.83 (bs, 1H), 4.12 (dd, J = 12.5, 5.3 Hz, 1H), 2.81 (m, 1H), 2.60 (m, 1H), 1.39 (s, 9H); ^{13}C NMR (400 MHz, DMSO-d_6; mixture of rotamers) δ: 175.4, 152.2, 150.9, 129.8, 106.1, 105.7, 78.8, 78.5, 60.2, 59.8, 35.7, 34.6, 28.1. Anal. Calcd for $C_{10}H_{14}LiNO_4 \cdot H_2O$: C, 50.64; H, 6.80; Li, 2.93; N, 5.91. Found: C, 50.31; H, 7.05; Li, 3.17; N, 6.24.

Preparation of (2*S*)-2-Carbamoyl-2,3-dihydropyrrole-1-carboxylic Acid *tert*-Butylester (1a). Lithium carboxylate **5b** (2.7 g, 12.5 mmol), CDI (5.1 g, 31.2 mmol), and AcOEt (27 mL) were charged to a round bottomed flask under nitrogen. The resulting mixture was cooled to 8 °C and stirred at the same temperature for 15 min. At this point, TFA (1.4 g, 12.5 mmol) was charged over 1 h keeping the temperature below 12 °C to minimize racemization and control CO_2 evolution. After aging for 1 h at 8 °C, formation of the intermediate acyl imidazole **6b** was confirmed by HPLC. The light brown mixture was cooled to 0−5 °C and an aqueous solution of NH_4OH (28 wt %, 2.4 g, 18.7 mmol) was added in less than 10 min while maintaining the reaction temperature at 0−20 °C. Thirty minutes after the addition of NH_4OH, the mixture was cooled to −5−0 °C and an aqueous solution of citric acid (56.2 mmol) was charged maintaining the temperature below 10 °C. After stirring for 15 min at 10 °C, the layers were separated, the aqueous layer was extracted with AcOEt, and the organic layers were combined. The combined organic extract was sequentially washed with citric acid in water (6.2 mmol), TMEDA (18.7 mmol), aqueous NaOH (0.5 N, 2 vol), and aqueous NaCl (25 wt %, 4 vol). The organic layer was distilled (ca. 25−30 °C, 100 mbar) to a volume of ca. 10 mL, filtered through a G-60 charcoal cartridge and further distilled to ca. 4.6 mL. Crystallization by addition of antisolvent cyclohexane in 2 portions of 7.8 g and seeding at 25 °C afforded a slurry that was cooled to 0−5 °C and held for 4 h. The slurry was filtered and rinsed with a mixture of AcOEt in cyclohexane (10 vol %) to afford dihydropyrrole **1a** as a tan solid (1.75 g, 70% yield, 99% ee). IR (DMSO) 3500 (NH_2), 1702, 1675 (C═O) cm^{-1}; ^{1}H NMR (400 MHz, DMSO-d_6; major rotamer) δ: 7.38 (s, 1H, H_2NCO), 6.98 (s, 1H, H_2NCO), 6.51 (bs, 1H, 5-H), 4.96 (bs, 1H, 4-H), 4.37 (dd, J = 11.5, 5.0 Hz, 1H, 2-H), 2.93 (m, 1H, 3-H), 2.44 (m, 1H, 3-H), 1.38 (s, 9H, $(CH_3)_3OCO$); ^{13}C NMR (400 MHz, DMSO-d_6; mixture of rotamers) δ: 173.4, 173.0, 151.2, 150.8, 129.9, 129.8, 105.8, 79.7, 79.5, 58.5, 58.2, 35.9, 34.7, 28.0, 27.9; HRMS (ESI-QTOF) calculated for $C_{10}H_{17}N_2O_3$ [M + H$^+$] 213.1239; found 213.1245.

Preparation of (1*S*, 3*S*, 5*S*)-3-(Aminocarbonyl)-2-azabicyclo-[3.1.0]hexane-2-carboxylic *tert*-butylester (2). Dihydropyrrole **1a** (12.0 g, 56.6 mmol) was dissolved in AcOEt (120 mL) in a round bottomed flask purged with nitrogen. CH_2I_2 (31.8 g, 119 mmol) was charged to the flask followed by water (0.18 g, 10.0 mmol) and the resulting mixture was cooled to −10 °C. Et_2Zn (15 wt % in toluene, 97.8 g, 119 mmol) was slowly added over 1 h while maintaining the temperature between 0 and −10 °C, and the reaction was held with agitation between 0 and −10 °C for 45 min. Then, a solution of TFA (3.22 g, 0.5 equiv) in toluene (10 g) was added over 10 min while maintaining the batch temperature between 0 and −10 °C. The reaction was warmed to 16 °C over 1 h and held for at least 30 min prior to quenching. A quench slurry consisting of disodium EDTA (31 g) in water (180 g) was prepared in a second flask at 15 °C and the reaction was transferred into the quench solution maintaining the internal temperature below 23 °C. Following the quench, the pH of the solution was brought to 6−6.5 by dosing 1 N NaOH. The quenched reaction was then heated to 50 °C, the agitation was stopped, and the solution was allowed to settle over 30 min before the bottom layer was removed. The aqueous layer was extracted with AcOEt (119 mL) and combined with the rich organic layer. Water (12 g) was added to the combined organic layers followed by TMEDA (3.3 g). The resulting biphasic solution was agitated for 15 min prior to separating the bottom layer to waste. An aqueous solution of NaOH (0.5 N, 11 g) was added to the mixture and agitated for 15 min prior to the addition of aqueous NaCl (25 wt %%, 11 g). The mixture was agitated for 15 min, allowed to settle for at least 30 min, and the bottom layer was separated to waste. The reaction was then distilled under vacuum to 72 mL, and *i*-PrOH (82 g) and water (54 g) were added to the reactor. The mixture was concentrated to 72 mL under vacuum, and the resulting slurry was heated to 65 °C for 30 min followed by a 2 h cooling ramp to 20 °C. After holding for 60 min at 20 °C, the batch was then cooled to 0−5 °C over 2 h and held for at least 6 h. The slurry was filtered, and the cake was washed with a mixture of *i*-PrOH (3.4 g) and water (24 g) kept at 0−5 °C. The cake was washed with *t*-BuOMe (12 g × 2) at the same temperature and dried under vacuum at 50 °C with a nitrogen sweep to afford L-*cis*-4,5-methanoprolinamide **2** as a white solid (9.0 g, 70% yield, >99.8% ee).

IR Experiments. IR spectra were recorded using a ReactIR spectrometer fitted with an 18-bounce silicon-tipped probe. The IR probe was inserted through a nylon adapter and TFE O-ring seal into a Schlenk flask fitted with a magnetic stir bar. After the flask was heated under vacuum and flushed with nitrogen, background and solvent reference spectra were recorded at 0 °C. The solvent was removed via syringe, the flask was heated and dried under vacuum, and a solution of dihydropyrrole **1a** in dry AcOEt was transferred via syringe to the IR

dx.doi.org/10.1021/jo500966m | J. Org. Chem. 2014, 79, 6233−6243

vessel and cooled to 0 °C in a thermostated bath for 30 min. Following an initial period of signal stabilization, spectra were recorded every 30 s at a gain of 1 and a resolution of 4 cm^{-1} over the course of the reactions with Et_2Zn (1.1 M in toluene) or $Zn(CH_2I)_2$ (0.64 M in AcOEt-toluene).

Kinetics. A solution of zinc amidate **7a** containing anhydrous *o*-xylene (0.041 M) as an HPLC standard was charged to an oven-dried, nitrogen-flushed 20 mL reaction vial fitted with a TFE septum and a stir bar. The vial was brought to the desired temperature using a thermostated bath (±0.2 °C), and the reaction was initiated by rapid injection of a stock solution of $Zn(CH_2I)_2$ (0.64 M in AcOEt-toluene) under a positive pressure of nitrogen.[51] Aliquot portions (0.1 mL) were periodically taken and quenched with 1:1 H_2O-ACN (1 mL) at intervals chosen to ensure an adequate sampling of the first 0−15% conversion, and analyzed using HPLC. The reactions were monitored by following the decay of the substrates and the formation of products relative to the internal *o*-xylene standard. Following the formation of the products afforded initial rates that were equivalent to those obtained by monitoring substrate decays within ±10%. The rates depicted in Figure 4 represent the average of two runs as determined using nonlinear least-squares analysis. The rates were reproducible within ±10%, and the errors reported in Supporting Information correspond to one standard deviation.

■ ASSOCIATED CONTENT

Supporting Information

General methods, copies of spectra, rate data, and molecular modeling coordinates. This material is available free of charge via the Internet at http://pubs.acs.org.

■ AUTHOR INFORMATION

Corresponding Authors

*E-mail: antonio.ramirez1@bms.com.

*E-mail: truc.vu@bms.com.

Notes

The authors declare no competing financial interest.

■ ACKNOWLEDGMENTS

We thank Gregory Beutner, Martin Eastgate, Francisco González-Bobes, and Dimitri Skliar for helpful discussions during the preparation of the manuscript. We also acknowledge the contribution of Simon Leung to the process safety analysis of the cyclopropanation.

■ REFERENCES

(1) Urbach, H.; Henning, R.; Becker, R. Ger. Offen. 3,324,263, 1985.

(2) Pellicciari, R.; Arenare, L.; De Caprariis, P.; Natalini, B.; Marinozzi, M.; Gallic, A. *J. Chem. Soc., Perkin Trans. 1* **1995**, 1251−1257.

(3) (a) Hanessian, S.; Ninkovic, S.; Reinhold, U. *Tetrahedron Lett.* **1996**, *37*, 8971−8974. (b) Hanessian, S.; Reinhold, U.; Saulnier, M.; Ciaridge, S. *Bioorg. Med. Chem. Lett.* **1998**, *8*, 2123−2128. (c) Hanessian, S.; Buckle, R.; Bayrakdarian, M. *J. Org. Chem.* **2002**, *67*, 3387−3397.

(4) For recent examples, see: (a) Pack, S. K.; Tymonko, S.; Patel, B. P.; Natalie, K. J., Jr.; Belema, M. Preparation of Linked Bis-1H-benzimidazoles, Bis-1H-imidazoles, 1H-benzimidazole-1H-imidazole and Analogs End-capped with Amino Acid or Peptide Derivatives as Hepatitis C Virus Inhibitors. U.S. Pat. Appl. US 20110269956 A1. (b) Homma, M.; Miyazaki, T.; Oguro, Y.; Kurasawa, O. Preparation of (Pyrazol-4-yl)dihydrothienopyrimidinone Derivatives as Anticancer Agents. PCT Int. Appl. WO 2011102399 A1. (c) Kolczewski, S.; Pinard, E. Tetrahydropyran Derivatives as GlyT-1 Inhibitors and Their Preparation and Use for the Treatment of Schizophrenia. U.S. Pat. Appl. US 20110190349 A1. (d) Galemmo, R. A., Jr.; Artis, D. R.; Ye, X. M.; Aubele, D. L.; Truong, A. P.; Bowers, S.; Hom, R. K.; Zhu, Y.-L.; Neitz, R. J.; Sealy, J.; Adler, M.; Beroza, P.; Anderson, J. P. Preparation of Pteridinones as Polo-like Kinase Inhibitors for Treating Neurodegenerative Diseases and Cancers. PCT Int. Appl. WO 2011079114 A1.

(5) (a) Bassan, E. M.; Baxter, C. A.; Beutner, G. L.; Emerson, K. M.; Fleitz, F. J.; Johnson, S.; Keen, S.; Kim, M. M.; Kuethe, J. T.; Leonard, W. R.; Mullens, P. R.; Muzzio, D. J.; Roberge, C.; Yasuda, N. *Org. Process Res. Dev.* **2012**, *16*, 87−95. (b) Frantz, M.-C.; Pierce, J. G.; Pierce, J. M.; Kangying, L.; Qingwei, W.; Johnson, M.; Wipf, P. *Org. Lett.* **2011**, *13*, 2318−1321. (c) Anthes, R.; Benoit, S.; Chen, C.-K.; Corbett, E. A.; Corbett, R. M.; DelMonte, A. J.; Gingras, S.; Livingston, R. C.; Pendri, Y.; Sausker, J.; Soumeillant, M. *Org. Process Res. Dev.* **2008**, *12*, 178−182. (d) Zhuo, J.; Burns, D. M.; Zhang, C.; Xu, M.; Weng, L.; Qian, D.-Q.; He, C.; Lin, Q.; Li, Y.-L.; Shi, E.; Agrios, C.; Metcalf, B.; Yao, W. *Synlett* **2007**, *3*, 460−464.

(6) For a discussion on the scaleup of zinc carbenoid-mediated cyclopropanations, see: Repic, O. In *Principles of Process Research and Chemical Development in the Pharmaceutical Industry*; John Wiley & Sons: New York, 1997; pp 14−16.

(7) (a) Wittig, G.; Schwarzenbach, K. *Angew. Chem.* **1959**, *71*, 652. (b) Wittig, G.; Wingler, F. *Chem. Ber.* **1964**, *97*, 2139−2145. (c) Furukawa, J.; Kawabata, N.; Nishimura, J. *Tetrahedron Lett.* **1966**, 3353−3354. (d) Furukawa, J.; Kawabata, N.; Nishimura, J. *Tetrahedron* **1968**, *24*, 53−58.

(8) Magnin, D. R.; Robl, J. A.; Sulsky, R. B.; Augeri, D. J.; Huang, Y.; Simpkins, L. M.; Taunk, P. C.; Betebenner, D. A.; Robertson, J. G.; Abboa-Offei, B. E.; Wang, A.; Cap, M.; Xin, L.; Tao, L.; Sitkoff, D. F.; Malley, M. F.; Gougoutas, J. Z.; Khanna, A.; Huang, Q.; Han, S.-P.; Parker, R. A.; Hamann, L. G. *J. Med. Chem.* **2004**, *47*, 2587−2598.

(9) (a) Jones, G. S.; Savage, S. A.; Ivy, S.; Benitez, P. L.; Ramirez, A. *J. Org. Chem.* **2011**, *76*, 10332−10337. (b) Savage, S. A.; Jones, G. S.; Kolotuchin, S.; Ramrattan, S. A.; Vu, T.; Waltermire, R. E. *Org. Process Res. Dev.* **2009**, *13*, 1169−1176. (c) Augeri, D. J.; Robl, J. A.; Betebenner, D. A.; Magnin, D. R.; Khanna, A.; Robertson, J. G.; Wang, A.; Simpkins, L. M.; Taunk, P.; Huang, Q.; Han, S.-P.; Abboa-Offei, B.; Cap, M.; Xin, L.; Tao, L.; Tozzo, E.; Welzel, G. E.; Egan, D. M.; Marcinkeviciene, J.; Chang, S. Y.; Biller, S. A.; Kirby, M. S.; Parker, R. A.; Hammann, L. G. *J. Med. Chem.* **2005**, *48*, 5025−5037. (d) Vu, T. C.; Brzozowski, D. B.; Fox, R.; Godfrey, J. D.; Hanson, R. L.; Kolotuchin, S. V.; Mazzullo, J. A.; Patel, R. N.; Wang, J.; Wong, K.; Yu, J.; Zhu, J.; Magnin, D. R.; Augeri, D. J.; Hamann, L. G. Methods and Compounds Producing Dipeptidyl Petidase IV Inhibitors and Intermediates Thereof. Int. Pub. Num. WO2004052850, 2004. (e) Hanson, R. L.; Goldberg, S. L.; Brzozowski, D. B.; Tully, T. P.; Cazzulino, D.; Parker, W. L.; Lyngberg, O. K.; Vu, T. C.; Wong, M. K.; Patel, R. N. *Adv. Synth. Catal.* **2007**, *349*, 1369−1378.

(10) Reactions decelerated by the induction period resulted in lower yields due to the competitive decomposition of the zinc carbenoid with a half life of approximately 60 h at 20 °C ($[Zn(CH_2I)_2]$ = 0.64 M, [AcOEt] = 4.85 M in toluene). For a related discussion, see: Voituriez, A.; Zimmer, L. E.; Charette, A. *J. Org. Chem.* **2010**, *75*, 1244−1250.

(11) Hanson, R. L.; Johnston, R. M.; Goldberg, S. L.; Parker, W. L.; Patel, R. N. *Enzyme Microb. Technol.* **2011**, *48*, 445−453.

(12) Yu, J.; Vu, T.; Riebel, P.; Hierla, E.; Mudryk, B. *Tetrahedron Lett.* **2005**, *46*, 4011−4013.

(13) Gill, I.; Patel, R. *Bioorg. Med. Chem. Lett.* **2006**, *16*, 705−709.

(14) Kunishima, M.; Kawachi, C.; Hioki, K.; Terao, K.; Tani, S. *Tetrahedron* **2001**, *57*, 1551−1558.

(15) The preparation of halomethylzinc reagents from Et_2Zn and CH_2I_2 enables an accurate control of the reagent stoichiometries, affords homogeneous solutions, and minimizes Schlenk-type equilibria: Denmark, S. E.; Edwards, J. P.; Wilson, S. R. *J. Am. Chem. Soc.* **1991**, *113*, 723−725.

(16) AcOEt was chosen on the basis of the limited solubility of **1a** and the overall process performance, including reaction conversion, purity, and recovery of 4,5-methanoprolinamide **2**. For a recent study of the solvent effect on cyclopropanations mediated by zinc carbenoids, see: Fujii, K.; Shiine, K.; Misaki, T.; Sugimura, T. *Appl. Organomet. Chem.* **2013**, *27*, 69−72. See also ref 7d.

(17) For diastereoselective cyclopropanations directed by −NHCOR moieties, see: (a) Csatayová, K.; Davies, S. G.; Lee, J. A.; Ling, K. B.; Roberts, P. M.; Russell, A. J.; Thomson, J. E. *Org. Lett.* **2010**, *12*, 3152−3155. (b) Csatayová, K.; Davies, S. G.; Lee, J. A.; Ling, K. B.; Roberts, P. M.; Russell, A. J.; Thomson, J. E. *Tetrahedron* **2010**, *66*, 8420−8440. (c) Davies, S. G.; Ling, K. B.; Roberts, P. M.; Russell, A. J.; Thomson, J. E. *Chem. Commun.* **2007**, 4029−4031. For reviews on directed cyclopropanations, see: (d) Charette, A. B.; Marcoux, J.-F. *Synlett* **1995**, 1197−1207. (e) Hoveyda, A. H.; Evans, D. A.; Fu, G. C. *Chem. Rev.* **1993**, *93*, 1307−1370.

(18) We represent Furukawa's reagent as $EtZnCH_2I$ for simplicity. Spectroscopic studies, however, have revealed that $EtZnCH_2I$ is in equilibrium with Et_2Zn and $Zn(CH_2I)_2$: (a) Charette, A. G.; Marcoux, J.-F. *J. Am. Chem. Soc.* **1996**, *118*, 4539−4549. (b) Denmark, S. E.; O'Connor, S. P. *J. Org. Chem.* **1997**, *62*, 3390−3401.

(19) For a recent review on the dynamic behavior of organozinc compounds, see : Guijarro, A. In *The Chemistry of Organozinc Compounds*; Rappoport, Z., Marek, I., Eds.; Wiley: Chichester, 2007; Chapter 6.

(20) The ethane resonance at 7.0 ppm could be detected by ^{13}C NMR spectroscopy at −10 °C.

(21) (a) Noltes, J. G.; Boersma, J. *J. Organomet. Chem.* **1969**, 345−355. (b) Coates, G. E.; Ridley, D. *J. Chem. Soc.* **1966**, 1065−1069.

(22) (a) Schmidt, S.; Schäper, R.; Schulz, S.; Bläser, D.; Wölper, C. *Organometallics* **2011**, *30*, 1073−1078. (b) Nishat, N.; Haq, M. M.; Ahamad, T.; Kumar, V. *J. Coord. Chem.* **2007**, *60*, 85−96. (c) Kleinpeter, E.; Ströhl, D.; Jovanovski, G.; Šoptrajanov, B. *J. Mol. Struct.* **1991**, *246*, 185−188.

(23) Charette, A. B.; Marcoux, J.-F. *J. Am. Chem. Soc.* **1998**, *120*, 5114−5115.

(24) For IR spectra assignments of CH_2I_2 and CD_2I_2, see: Ford, T. A. *J. Mol. Spectrosc.* **1975**, *58*, 185−193.

(25) The problematical insertion of CH_2I_2 into related ROZnEt species compared with $ZnEt_2$ has been noted previously: Charette, A. B.; Brochu, C. *J. Am. Chem. Soc.* **1995**, *117*, 11367−11368.

(26) Such exchange would afford mixtures of iodomethylzinc amidate **8b**, $Zn(CH_2I)_2$ and $EtZnCH_2I$ that, by analogy with the rapid reactivity of Et_2Zn with the first and second equivalent of CH_2I_2, could consume the excess CH_2I_2 allowing for formation of **8b** and $Zn(CH_2I)_2$. For a review, see: Blake, A. J.; Shannon, J.; Stephens, J. C.; Woodward, S. *Chem.—Eur. J.* **2007**, *13*, 2462−2472.

(27) ^{13}C NMR spectra of samples containing Et_2Zn (0.15 M) and 2 equiv $^{13}CH_2I_2$ prepared at 0 °C in AcOEt also showed the same resonance at −17.3 ppm. For ^{13}C NMR spectroscopic studies on $Zn(CH_2I)_2$, see refs 15 and 18.

(28) (a) Charette, A. B.; Molinaro, C.; Brochu, C. *J. Am. Chem. Soc.* **2001**, *123*, 12160−12167. (b) Charette, A. B.; Marcoux, J.-F.; Molinaro, M.; Beauchemin, A.; Brochu, C.; Élise, I. *J. Am. Chem. Soc.* **2000**, *122*, 4508−4509. (c) Charette, A. B.; Marcoux, J.-F.; Belanger-Gariepy, F. *J. Am. Chem. Soc.* **1996**, *118*, 6792−6793. Dimer: Lacasse, M.-C.; Poulard, C.; Charette, A. B. *J. Am. Chem. Soc.* **2005**, *127*, 12440−12441.

(29) Zinc amide aggregates: (a) Schmidt, S.; Schäper, R.; Schulz, S.; Bläser, D.; Wölper, C. *Organometallics* **2011**, *30*, 1073−1078. (b) Long, J.; Xu, L.; Du, H.; Li, K.; Shi, Y. *Org. Lett.* **2009**, *11*, 5226−5229. (c) Noltes, J. G.; Boersma, J. *J. Organomet. Chem.* **1969**, *16*, 345−355.

(30) Zinc complexes and reactions are routinely influenced by the aggregation of the zinc intermediates in solution: (a) Noyori, R.; Suga, S.; Kawai, K.; Okada, S.; Kitamura, M. *Pure Appl. Chem.* **1988**, *60*, 1597−1606. (b) Rosner, T.; Sears, P. J.; Nugent, W. A.; Blackmond, D. G. *Org. Lett.* **2000**, *2*, 2511−2513. (c) Blackmond, D. G.; McMillan, C. R.; Ramdeehul, S.; Schorm, A.; Brown, J. M. *J. Am. Chem. Soc.* **2001**, *123*, 10103−10104. (d) Buono, F.; Walsh, P. J.; Blackmond, D. G. *J. Am. Chem. Soc.* **2002**, *124*, 13652−13653. (e) Wipf, P.; Jayasuriya, N.; Ribe, S. *Chirality* **2003**, *15*, 208−212. (f) Brown, J. M.; Gridnev, I.; Klankermayer, J. *Top. Curr. Chem.* **2008**, *284*, 35−65. (g) Ercolani, G.; Schiaffino, L. *J. Org. Chem.* **2011**, *76*, 2619−2626.

(31) IR bands corresponding to the AcOEt solvent were subtracted following a background replacement and the spectra were baseline corrected at 1660 cm^{-1}.

(32) Iodine was described by Glukhovtsev's modification of the 6-311G basis set: (a) Glukhovtsev, M. N.; Pross, A.; McGrath, M. P.; Radom, L. *J. Chem. Phys.* **1995**, *103*, 1878−1885. (b) Glukhovtsev, M. N.; Pross, A.; McGrath, M. P.; Radom, L. *J. Chem. Phys.* **1996**, *104*, 3407. This basis set has been previously applied to the study of cyclopropanations mediated by zinc carbenoids: (c) Eger, W. A.; Zercher, C. K.; Williams, C. M. *J. Org. Chem.* **2010**, *75*, 7322−7331.

(33) We hasten to note that, in the absence of experimental data on the aggregation of **7a**, the choice of implicit solvation and monomeric species provides results that must be interpreted as general trends rather than definite values. For a general review on the impact of aggregation upon reactivity, see: McNeil, A. J.; Ramirez, A.; Collum, D. B. *Angew. Chem., Int. Ed.* **2007**, *46*, 3002−3017.

(34) Solvated analogues of structure **10** ($n \neq 0$) and complexes **11**−**16** could not be located presumably owing to steric hindrance.

(35) Bissette, A. J.; Fletcher, S. P. *Angew. Chem., Int. Ed.* **2013**, *52*, 2−30.

(36) Likewise, the addition of 20% v/v of an ended reaction to the reaction between **7a** and $Zn(CH_2I)_2$ mediated the loss of the sigmoidal profile and accelerated the cyclopropanation. See Supporting Information for details.

(37) Espenson, J. H. In *Chemical Kinetics and Reaction Mechanisms*; McGraw-Hill: New York, 1995; pp 7−81.

(38) A first-order dependence on the concentration of zinc carbenoid has been reported previously: Blanchard, E. P.; Simmons, H. E. *J. Am. Chem. Soc.* **1964**, *86*, 1347−1356.

(39) Nakamura, M.; Hirai, A.; Nakamura, E. *J. Am. Chem. Soc.* **2003**, *125*, 2341−2345.

(40) Boersma, J. In *Comprehensive Organometallic Chemistry*; Wilkinson, G., Ed.; Pergamon Press: New York, 1984: Vol. 2, Chapter 16.

(41) From Sigma-Aldrich: ≥99.99% ZnI_2, 25 g, $143.50 (230014).

(42) (a) Cheng, D.; Huang, D.; Shi, Y. *Org. Biomol. Chem.* **2013**, *11*, 5588−5591. (b) Lorenz, J. C.; Long, J.; Yang, Z.; Xue, S.; Xie, Y.; Shi, Y. *J. Org. Chem.* **2004**, *69*, 327−334. (c) Charette, A. B.; Beauchemin, A.; Francoeur, S. *J. Am. Chem. Soc.* **2001**, *123*, 8139−8140. (d) Yang, Z.; Lorenz, J. C.; Shi, Y. *Tetrahedron Lett.* **1998**, *39*, 8621−8624.

(43) Anderson, N. G. In *Practical Process Research and Development*; Academic Press: New York, 2000.

(44) (a) For a recent discussion of the effect of zinc oxo-complexes derived from water on related reactions, see: Fandrick, D. R.; Reeves, J. T.; Bakonyi, J. M.; Nyalapatla, P. R.; Tan, Z.; Niemeier, O.; Akalay, D.; Fandrick, K. R.; Wohlleben, W.; Ollenberger, S.; Song, J. J.; Sun, X.; Qu, B.; Haddad, N.; Sanyal, S.; Shen, S.; Ma, S.; Byrne, D.; Chitroda, A.; Fuchs, V.; Narayanan, B. A.; Grinberg, N.; Lee, H.; Yee, N.; Brenner, M.; Senanayake, C. H. *J. Org. Chem.* **2013**, *78*, 3592−3615 and references cited therein..

(45) Richards, P. I.; Boomishankar, R.; Steiner, A. *J. Organomet. Chem.* **2007**, 2773−2779.

(46) (a) Noltes, J. G.; Boersma, J. *J. Organomet. Chem.* **1968**, *12*, 425. (b) Inoue, S.; Kobayashi, M.; Tozuka, T. *J. Organomet. Chem.* **1974**, *81*, 17−21.

(47) For general discussions on the effect of Lewis acids on cyclopropanations, see: (a) Cornwall, R. G.; Wong, O. A.; Du, H.; Ramirez, T. A.; Shi, Y. *Org. Biomol. Chem.* **2012**, *10*, 5498−5513. (b) Charette, A. B. In *The Chemistry of Organozinc Compounds*; Rappoport, Z., Marek, I., Eds.; Wiley: Chichester, 2007; Chapter 7. (c) Denmark, S. E.; Beutner, G. In *Cycloaddition Reactions in Organic Synthesis*; Kobayashi, S., Jørgensen, K. A., Eds.; Wiley-VCH: Weinheim, 2002; pp 85−150. (d) Charette, A. B.; Beauchemin, A. *Org. React.* **2004**, *58*, 1−415. (e) Lebel, H.; Marcoux, J.-F.; Molinaro, C.; Charette, A. B. *Chem. Rev.* **2003**, *103*, 977−1050.

(48) Christoffers, J.; Koripelly, G.; Rosiak, A.; Rössle, M. *Synthesis* **2007**, *9*, 1279−1300.

(49) (a) Simmons, H. E.; Smith, R. D. *J. Am. Chem. Soc.* **1958**, *80*, 5323. (b) Simmons, H. E.; Smith, R. D. *J. Am. Chem. Soc.* **1959**, *81*, 4256.
(50) Krasovskiy, A.; Knochel, P. *Synthesis* **2006**, 890−891.
(51) Monitoring the formation of the $Zn(CD_2I)_2$ under an oxygenated atmosphere (1% in nitrogen) did not affect the rates of cyclopropanation. Oxygen has been reported to accelerate the Simmons-Smith reaction: (a) Miyano, S.; Hashimoto, H. *Chem. Commun.* **1971**, 1418−1300. (b) Miyano, S.; Hashimoto, H. *Bull. Chem. Soc. Jpn.* **1973**, *46*, 892−897.